

# Temporal and Spatial Characteristics of Intraseasonal Oscillations in the Meridional Wind Field over the Subtropical Northern Pacific\*

HAN Rongqing<sup>†</sup> (韩荣青), LI Weijing (李维京), and DONG Min (董敏)

National Climate Center, China Meteorological Administration, Beijing 100081

(Received January 17, 2009; revised March 25, 2010)

## ABSTRACT

Based on the NCEP/NCAR reanalysis I daily data from 1958 to 2002, climatic characteristics of the 30–60-day intraseasonal oscillations (ISOs) of the zonal wind ( $u$ ), meridional wind ( $v$ ), and geopotential height ( $h$ ) over global areas and especially the ISO of  $v$  over the subtropical northern Pacific are analyzed using the space-time spectrum analysis and wavelet transform methods. The results show that the ISO of  $v$  is very different from those of  $u$  and  $h$ , with the former representing the meridional low-frequency disturbances, which are the most active in the subtropics and mid-high latitudes, but very weak in the tropics. In the subtropical Northern Hemisphere, the energies of the ISOs of  $u$  and  $h$  are both concentrated on the waves with wave number of 1 and periods of 30–60 days, while the main energy of the ISO of  $v$  is concentrated on the waves with wave numbers of 4–6 and periods of 30–60 and 70–90 days. The westward propagating energies for the 30–60-day oscillations of  $u$ ,  $v$ , and  $h$  are all stronger than the eastward propagating energies in the subtropics. In addition, the ISO of  $v$  is the strongest (weakest) in summer (winter) over the subtropics of East Asia and northwestern Pacific, while the situation is reversed over the subtropical northeastern Pacific, revealing a “seesaw” of the ISO intensity with seasons over the subtropics from the northwestern to northeastern Pacific. In the subtropical northwestern Pacific, the interannual and interdecadal changes of the ISO for  $v$  at 850 hPa indicate that its activities are significantly strong during 1958–1975, while obviously weak during 1976–1990, and are the strongest during 1991–2000, and its spectral energy is obviously abnormal but ruleless during the ENSO periods. However, in the 2–7-yr band-pass filtering series, the interannual changes of the  $v$  ISO over the subtropical northwestern Pacific contain distinct ENSO signals. And in the 9-yr low-pass filtering series, the  $v$  ISO changes over the subtropical northwestern Pacific are significantly out of phase with the changes of the Niño-3.4 SST, whereas the  $v$  ISO changes in the subtropical northeastern Pacific are significantly in phase with the changes of the Niño-3.4 SST.

**Key words:** subtropics, meridional wind, intraseasonal oscillation (ISO), climate characteristics

**Citation:** Han Rongqing, Li Weijing, and Dong Min, 2010: Temporal and spatial characteristics of intraseasonal oscillations in the meridional wind field over the subtropical northern Pacific. *Acta Meteor. Sinica*, **24**(3), 276–286.

## 1. Introduction

People’s understanding of the extratropical 30–60-day intraseasonal oscillations (ISOs) is still poor, especially the independence and importance of ISO in the subtropics, though there are a lot of studies (Madden and Julian, 1971, 1972) on the climate characteristics of the tropical MJO (Madden and Julian oscillation). Comprehensive research on space-time characteristics of the subtropical ISO is lacking. A number of studies (e.g., Krishnamurti and Gadgil, 1985) have proved that ISO exists in the extratropics. Ini-

tially, the extratropical ISO was interpreted as a kind of response to the forcing from the tropical ISO (Anderson and Rosen, 1983; Magana and Yanai, 1991). However, a large number of investigations reveal that the extratropical low-frequency oscillations are different from the MJO in the tropics and have their own independent origins (Liebmann and Hartmann, 1984; Murakami, 1988; Hsu et al., 1990). Simmons et al. (1983) found that linear unstable waves with a period of about 50 days exist in the barotropic linear pattern of 300-hPa circulation in the Northern Hemisphere in winter, and they believed that the energy of the

\*Supported jointly by the National Basic Research Program of China (2006CB403606), the National Natural Science Foundation of China (Grant Nos. 40575027 and 40905035), and the National Non-Profit Public-Interest Research Project (Grant No. GYHY200806004).

<sup>†</sup>Corresponding author: hrq@cma.gov.cn.

extratropical ISO comes from the unstable barotropic mode of the basic flow. The studies of Ghil and Mo (1991) and Jin and Ghil (1990) both showed that the interactions between the large-scale disturbances in the extratropics and the topographic forcing can give rise to ISO. Dickey et al. (1991) found that the ISO of the atmospheric relative angular momentum in midlatitudes of the Northern Hemisphere shows an attribute of propagating to the equator, indicating that the ISO exists independently in the extratropics and it can influence the tropical atmosphere. The research of Chinese scholars also showed the independence and importance of the subtropical ISO in East Asia (Chen and Xie, 1988; He and Yang, 1992; Sun and Chen, 1988; Xu et al., 1999). Relevant studies revealed that the 30–60-day atmospheric oscillations in the subtropical East Asia in summer mainly propagate westward (Chen and Xie, 1988). On the other hand, the subtropical East Asia is where the ISO propagating northward converges with the ISO propagating southward (He and Yang, 1992). Moreover, special ISO activities exist over the Tibetan Plateau (Sun and Chen, 1988), and their frequency and amplitude are related to the stability of the atmosphere and the topographic forcing of the plateau (Xu et al., 1999), in which the topographic differences make the frequency discrepancy in the meridional propagation of ISO over the southern and northern slopes of the plateau.

The ISO activities in the subtropical northern Pacific directly influence the summer drought/flood in eastern China (Li, 1992; Chen et al., 2001; Han et al., 2006). For example, during the flood season in North China, the ISO in the northwestern Pacific is stronger; while under drought conditions, the ISO there is weaker (Li, 1992). The 1998 summer great flood in the mid and lower reaches of the Yangtze River is related to frequent ISOs propagating westward from the northwestern Pacific (Chen et al., 2001). Han et al. (2006) studied the summer drought/flood occurrences in eastern China during 1958–2000, and found that when heavy precipitation took place, the westward propagation of ISO in the meridional wind ( $v$ ) field from the northwestern Pacific along the same latitudes was active; but when drought conditions dominated,

the westward propagation of ISO was weak or even interrupted. Recent research (Ju et al., 2007) showed that the northward summer monsoon surges from the tropical South Asia combined with the zonal propagating ISO from the northwestern Pacific can lead to heavy precipitation in the mid and lower reaches of the Yangtze and Huai River basins, and moreover, the zonal propagating ISOs are likely to control the position of the large-scale rain band in China.

An important investigation revealed the global kinetic energy distributions of the zonal mean ISO (Li, 1993). But the ISO discrepancies at different zones after removing the latitude differences are still not clear. Therefore, the basic elements such as wind and geopotential height are standardized in our study in advance, and the space-time characteristics of ISO in the meridional wind  $v$  are analyzed and compared with those of other elements (zonal wind  $u$  and geopotential height  $h$ ) in this paper. In addition, different from most of the past ISO studies, the current study uses a two-dimensional space-time spectrum analysis method (Hayashi, 1982; Huang and Li, 1984; Chen et al., 2000) to do the filtering of data. Though past studies took into consideration the temporal fluctuation of variables at individual points of a space domain, they ignored the relationship between the fluctuations of each variable in the space and time series. The two-dimensional space-time spectrum analysis has a remedy for this and is advantageous to the understanding of the dynamic propagating characteristics of ISO. Dong et al. (2004) used this method to study the ISO space-time characteristics of 850-hPa zonal wind and OLR in the tropics, and found that in the active regions of MJO, such as the Indian Ocean and the tropical western Pacific, the MJO is the most active in summer, and it is fairly weak in spring and autumn.

Because the ISO sources in the extratropics and tropics are different and the activities of the ISO for  $v$  in the subtropical northern Pacific in summer have important influences on the drought/flood situation in eastern Asia (Han et al., 2006), and at present, understanding of the characteristics of the meridional low frequency disturbances in the wind field is still lacking, this paper employs the two-dimensional space-

time spectrum analysis and wavelet analysis methods to make an in-depth analysis of ISO over the subtropical Northern Hemisphere, especially the climate characteristics of the  $v$  ISO in the subtropical northern Pacific, and compares these with the climate characteristics of the ISO of other elements revealed by previous studies.

## 2. Data and methodology

The daily wind and height fields of NCEP/NCAR reanalysis data I (Kalnay et al., 1996) from 1958 to 2002 are used. The data have a horizontal resolution of  $2.5^\circ \times 2.5^\circ$ . At first, they are standardized for comparison of the ISO activities at different latitudes. Then the data are treated with pentad average in order to reduce the computation load in the space-time spectrum analysis and the wavelet analysis. The methods adopted in this paper are described as follows:

(1) Two-dimensional space-time spectrum analysis. The space-time spectrum of ISO is calculated by this method, and the paper analyzes the distributions of all kinds of variation energy based on the wave number and frequency, and verifies the main energy features of the traveling and standing waves on the intraseasonal time scale. Meanwhile, the paper uses this method to filter the original data, to keep the large-scale spatial fluctuations with wave numbers of 1–6, and to maintain the temporal oscillations with periods of 10–90 days.

(2) Wavelet analysis. The Fourier transform is used to spread the time series on the frequency domain, and translate the time series into the waves with different frequencies, and then deduce the mean energy of a time series for each frequency wave and its percentage to the total wave energy. However, the Fourier transform cannot offer the variation information of the energy of waves with time. Therefore, the wavelet analysis is used to open the frequency window of the element time series at some moments. The Morlet wavelet is used in this paper. The detailed calculation is carried out according to the method introduced by Torrence and Compo (1998).

(3) Band-pass and low-pass filtering. With the

fast Fourier transform filtering method, the paper obtains climatic information on the ENSO cycle time scale (2–7 yr) and the interdecadal time scale, based on the monthly Niño-3.4 SST departure index and the 30–60-day spectral energy time series drawn from the wavelet analysis.

## 3. The meridional intraseasonal disturbances in the subtropics

A two-dimensional space-time spectrum analysis has been conducted on the daily data series for each year and the spatial series at every grid along certain latitudes, for meridional wind speed ( $v$ ), zonal wind speed ( $u$ ), and height ( $h$ ) from 1958 to 2002. Note that for comparison of the space-time spectrum of the ISO at different latitudes, the data are firstly treated by standardization. After the space-time spectrum analysis, the percentage of 30–60-day ISO spectral energy (power spectrum or variance) to the total spectral energy (the sum of the spectral energies of all waves) of the atmosphere can be obtained, and is called the variance ratio or variance contribution rate. It should be noted that the result of the space-time spectrum analysis represents an average state of the space-time series (all days in one year and 144 grids along a latitude circle herein) according to the requirement to minimize boundary errors in the Fourier transform of the space-time spectrum analysis.

The distributions (figure omitted) of ISO variance ratios of  $u$ ,  $v$ , and  $h$  along separate latitudes at 850 and 200 hPa show that the variance ratios at high pressure levels are all bigger than those at lower pressure levels, and among them, the distributions of the variance ratios of  $u$  and  $h$  are similar: both of them are bigger in the equatorial belt and smaller in the subtropical zone. However, the ISO variance ratio of  $v$  exhibits peak values at the subtropical zone, and it is very weak at the equator and the zones around the equator. Therefore, it is inferred that the ISO of meridional disturbances in the wind field is active in the subtropics, but less energetic in the tropics.

Figure 1 shows the height-latitude variance ratio distributions of the 30–60-day oscillations of  $u$  and  $v$ .

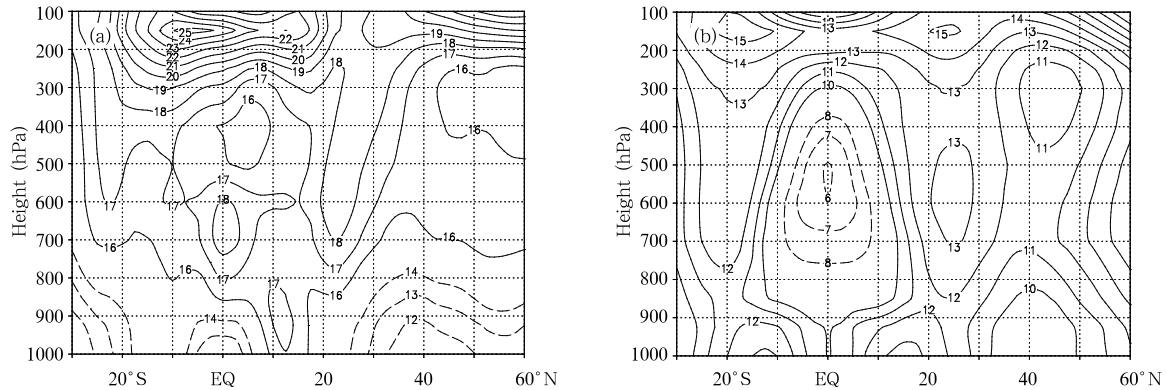


Fig. 1. Height-latitude sections of ISO variance ratios of normalized (a) zonal wind and (b) meridional wind.

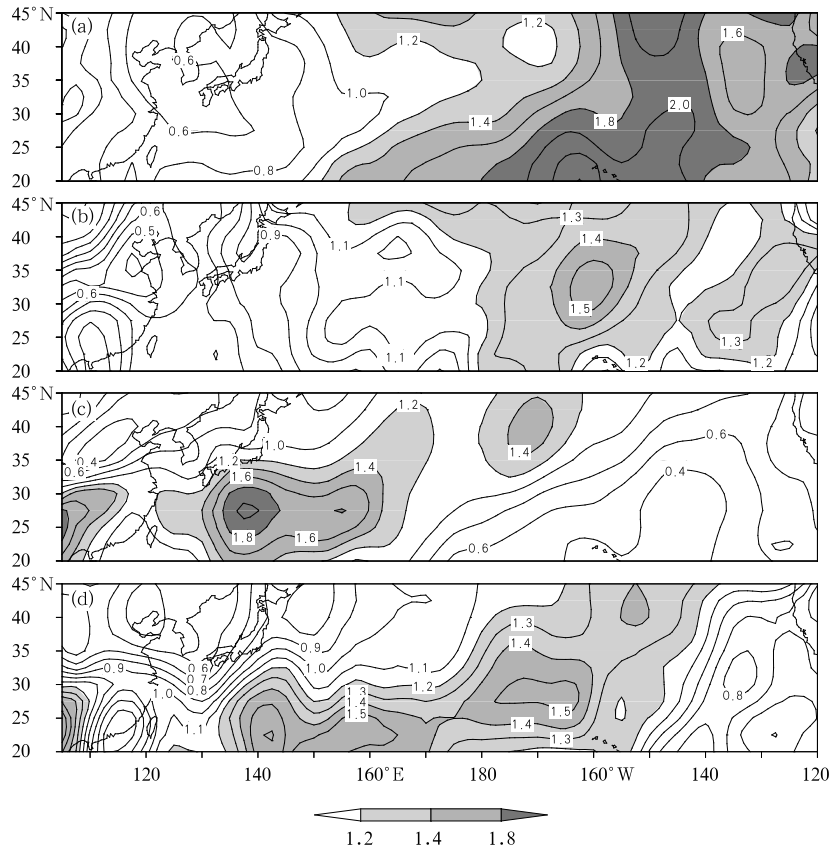
Considering the computation efficiency and the data discontinuity in the NCEP reanalysis around 1979, Fig. 1 represents the annual average situation during 1980–2002.

Figure 1a shows that the spectral energy of the  $u$  ISO in the troposphere is mainly distributed on the high levels above 300 hPa, in which the maximum variance ratios are located around the equator between  $20^{\circ}\text{S}$  and  $20^{\circ}\text{N}$  and with the center value above 25%, and the next high value center is located within  $40^{\circ}$ – $60^{\circ}\text{N}$ . On the low levels of the troposphere, the variance ratios of the  $u$  ISO reach maximum between  $22^{\circ}\text{S}$  and  $22^{\circ}\text{N}$ , and they are smaller in other latitudes, and remarkably small at lower levels between  $25^{\circ}$  and  $50^{\circ}\text{N}$ . The variance ratio distribution of the  $h$  ISO is similar with that of  $u$  (figure omitted). Different from that, on the mid and lower levels of the troposphere (Fig. 1b), the spectral energies of the  $v$  ISO are obviously smaller over the equator, and their variance ratios are mostly no more than 10% between  $10^{\circ}\text{S}$  and  $10^{\circ}\text{N}$ ; however, a high value center is found in the subtropical zone of  $20^{\circ}$ – $30^{\circ}\text{N}$  and the variance ratios are slightly lowered at  $30^{\circ}$ – $50^{\circ}\text{N}$ , but they are still higher than that over the equator. As in the  $u$  field, the variance ratios of the  $v$  ISO are also bigger on high levels than on low levels in the troposphere. In a word, for  $v$ , a variable representing the northward/southward disturbances of the wind field, the variance ratio distribution of its ISO with latitude is quite different from those of  $u$  and  $h$ .

## 4. Space-time characteristics of the subtropical ISO

### 4.1 Interseasonal variations

In this study, we analyze the standardized and pentad time series data of 850-hPa  $v$  from 1958 to 2002 using the Morlet wavelet method, and then obtain ISO wavelet energy (square of wave amplitude) in four seasons averaged for 45 yr, including winter (December, January, and February), spring (March–May), summer (June–August), and autumn (September–November). Figure 2 shows distributions of ISO wavelet energy of 850-hPa  $v$  for the four seasons in the subtropical regions from eastern Asia to Pacific. It is clear that the prevailing ISO gradually shifts between Northeast Pacific and Northwest Pacific with seasons (Fig. 2). The strongest ISO appears in summer in the subtropical regions from eastern Asia to northwestern Pacific. But as a whole, the strongest ISO wavelet energy appears in northeastern Pacific in winter. In the south of  $30^{\circ}\text{N}$  from eastern Asia to northwestern Pacific, ISO energy is the strongest in summer, followed by that in autumn, and it is the weakest in winter and spring. On the contrary, in the northeastern Pacific, ISO energy is the strongest in winter, the second strongest in spring, and the weakest in summer and the second weakest in autumn. Hence the variations of the  $v$  ISO intensity with seasons shifting in the two areas take on a “seesaw” pattern.



**Fig. 2.** Seasonal distributions of ISO wavelet power spectra averaged from 1958 to 2002 for normalized meridional wind at 850 hPa for (a) winter, (b) spring, (c) summer, and (d) autumn.

#### 4.2 The space-time spectrum structure of the zonally propagating ISO

Figure 3 shows the space-time spectra of 850-hPa  $h$ ,  $u$ , and  $v$  averaged between 20° and 30°N with a period range of 10–90 days and wave numbers of 1–8 (wave number 0 represents the zonal average, and will not be discussed in this paper). It represents the distribution structure of the ISO spectrum energy along an entire latitudinal circle averaged for 45 yr from 1958 to 2002. The left panels in Fig. 3 are for the waves propagating westward and the right panels for the waves propagating eastward. The wave components with the same wave number, same amplitude, and same frequency but opposite travel directions (eastward vs. westward) will form standing wave (Hayashi, 1982). When the ratio of the power spectra with the same wave number and the same period in the left and right panels is closer to 1, the proportion of the stand-

ing waves is bigger. Figures 3a–d show that 30–60-day low-frequency oscillations of  $h$  and  $u$  are comparatively significant with 10–90-day periods, and both have the biggest energy concentrated on the wave numbers 1–2, which is consistent with the past research results (Chen et al., 2000). The strength of eastward and westward propagating ISOs of  $h$  is somewhat similar to that of  $u$  in the wave numbers 1–2 and periods of 30–90 days (Figs. 3a, b). The strength of the westward propagating ISO of  $u$  is obviously stronger than that of its eastward propagating counterpart, and in the wave numbers 1–2, the fluctuation energy ratio of westward to eastward propagation spans from 5:4 to 2:1. This indicates that there are still some westward traveling waves in spite of the standing waves occupying an outstanding proportion (Figs. 3c, d). Figures 3e and 3f show that the spectrum structure of  $v$  in the low-frequency oscillations is very different, in which

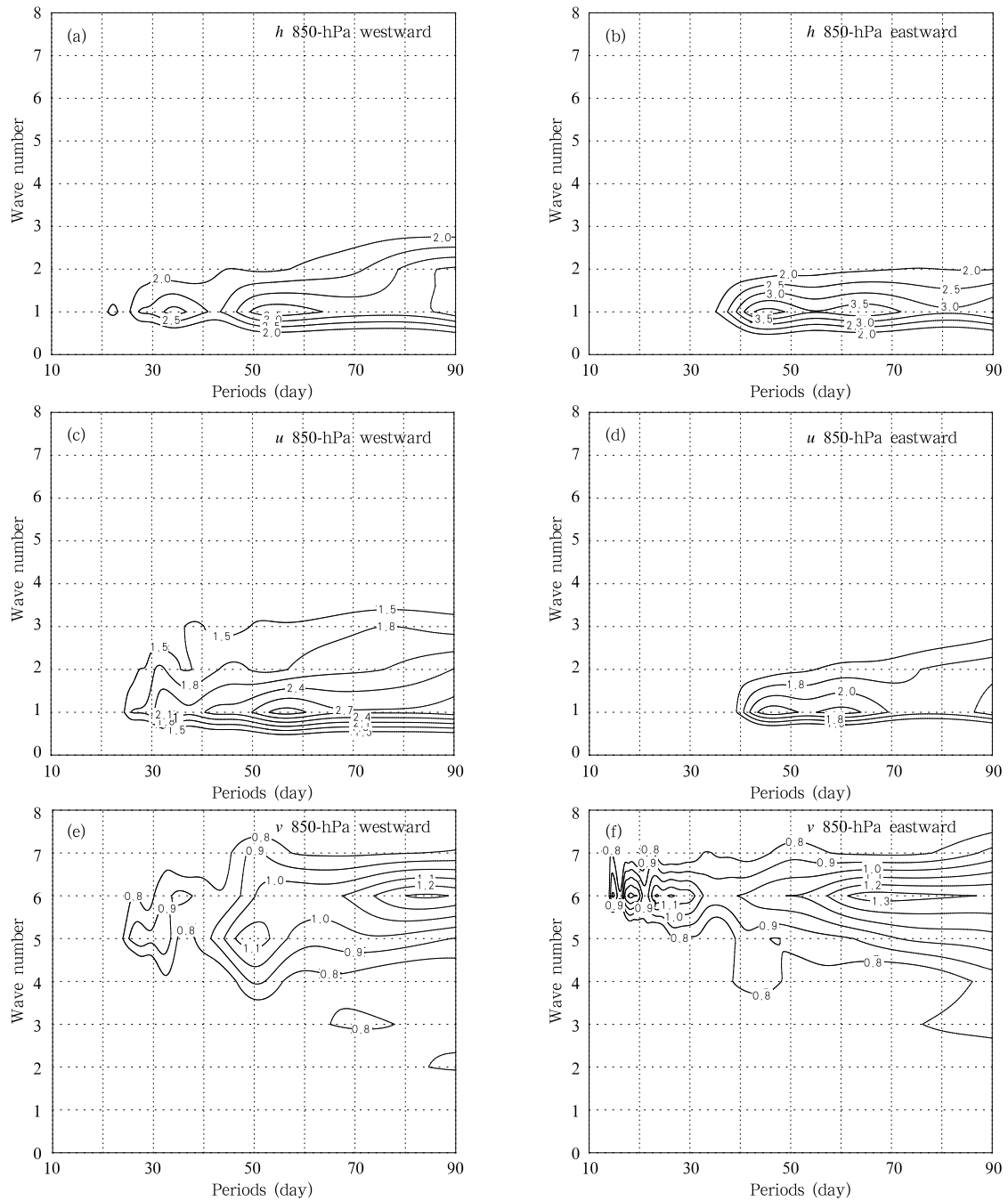


**Fig. 3.** Structures of the space-time power spectra of westward (left panels) and eastward (right panels) propagating waves for 850-hPa height (a, b), zonal (c, d) and meridional (e, f) winds during the period of 1958–2002 (power spectra times  $10^5$  and averaged between  $20^\circ$  and  $30^\circ$ N). All variables are standardized and 5-day averaged before the space-time spectrum analysis and smoothing.

the 30–60-day oscillations are also very prominent, and the biggest energy is concentrated on the wave numbers 5–6. This means that the space scale of the meridional fluctuations is smaller than that of either  $h$  or  $u$ ,

and it may be related to the discontinuous change of the meridional wind speed along the latitudinal circle. The westward propagation of the  $v$  ISO is obviously stronger than the eastward propagation, and

the ratio of the two also spans from 5:4 to 2:1. The space-time spectra of the variables averaged within  $32.5^{\circ}$ – $45.0^{\circ}$ N (figure omitted) are basically similar to the aforesaid spectrum structure of the intraseasonal waves in the subtropical zone, but the main energy of the  $v$  ISO is concentrated on the wave numbers 4–5, slightly lower than the wave numbers of the latter (between  $20^{\circ}$  and  $30^{\circ}$ N). This may be associated with the different meridional circulations distributed separately in the subtropics and midlatitudes. Since the quasi-stationary cyclonic and anticyclonic circulations like the subtropical high always appear in the subtropics but zonal flows frequently occur in midlatitudes, the zonal space scale of the meridional wind ISO in the subtropics is smaller. In general, there are four big troughs in the midlatitude westerlies in the mid troposphere in summer, and the ridge is not very obvious; while there are three troughs and three ridges in winter, so the zonal space scale of the midlatitude  $v$  ISO is bigger in winter. Besides, within  $32.5^{\circ}$ – $45.0^{\circ}$ N, for the  $v$  ISO, the westward propagating energy is also stronger than the eastward propagating energy, and the ratio of the two spans from 5:4 to 9:4, so the proportion of the standing waves is slightly smaller than the above-mentioned counterpart in the subtropics.

#### 4.3 Characteristics of the ISO daily evolution

In order to understand the influence of the ISO on the weather in the subtropical zone, we provide two representative examples of ISO influencing the weather in this region. Figure 4 shows a comparison of the daily evolution between the ISO of 850-hPa  $h$  and its original field without filtering. Only the ISO height contours with values above 0 are given in 1985, i.e., only the low-frequency high pressure systems are shown. While for 1998, only the ISO height contours with values below 0 are given, i.e., only the low pressure systems in the ISO height field are shown. On 1 July 1985 (Fig. 4a), there was a low-frequency high pressure system accompanying an original high pressure system, whose centers were located in the mid East Pacific, and the former moved westward later on 6 July (Fig. 4b), but the corresponding original high pressure system apparently moved southward. Then the two systems both moved westward obviously from

11 (Fig. 4c) through 16 July (Fig. 4d), so the original low pressure circulation (low-frequency low pressure omitted in the figures of 1985) located in the west of the high pressure system and accompanying it all the time, also moved westward and led to the anomalous precipitation in Japan and the continent of East Asia. For another example, as Figs. 4e–h show, on 16 June 1998, a small low-frequency cyclone was formed around east of the dateline and centered at  $25^{\circ}$ N, and subsequently it gradually shifted northwestward and enhanced constantly till it turned into a strong low-frequency cyclone dominating the mid-lower reaches of the Yangtze River and began to make large-scale heavy rain in the local region on 21 July (Fig. 4h). In general, Fig. 4 shows that the evolution of the low-frequency height field and the original height field are in the same direction when a strong rainfall case occurs; the ISOs only account for a small portion of the original field at the initial stage before a special weather process, but when the low-frequency system is vigorously flourishing, the characteristics of the original field and the low-frequency field become very similar (Han et al., 2006).

#### 4.4 Interannual/interdecadal variations of the subtropical ISO

The Morlet wavelet time-period power-spectra analysis (figure omitted) of 850-hPa  $v$  averaged over the subtropical eastern Asia ( $20^{\circ}$ – $30^{\circ}$ N,  $115^{\circ}$ – $130^{\circ}$ E) in the pentad data time series during 1958–2000 indicates that the wave spectrum energy with a 1-yr period is the most remarkable. The ISO, whose power spectrum has passed the 95% red noise reliability test, also exhibits an obvious decadal change. The ISO activities are considerably strong during 1958–1975, very weak during 1976–1990, and the strongest during 1991–2000.

The results of Dong et al. (2004) and Li and Li (1998) both showed that the 30–60-day tropical oscillations are considerably active during the La Niña periods, but very weak during the El Niño periods. The  $v$  ISO at 850 hPa over the subtropical northern Pacific also displays abnormal activities during the ENSO event, but their power spectrum variation is not definite during the El Niño/La Niña period. In order to further understand the subtropical ISO during

the ENSO cycles, we convert the pentad ISO wavelet power spectra of the 850-hPa  $v$  into monthly data for

43 yr to conform with the time scale of the monthly Niño-3.4 index of SST anomalies, and then carry out

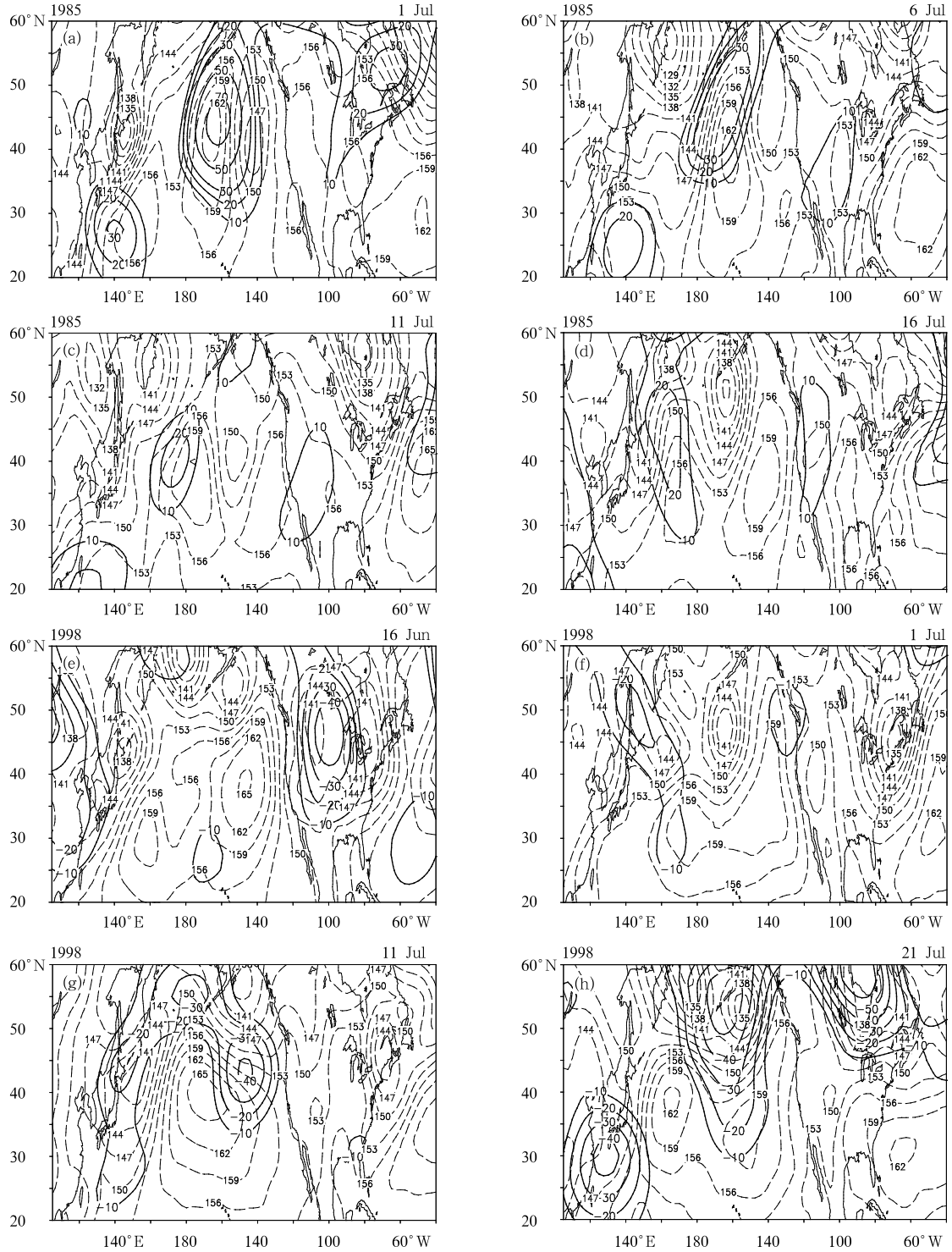


**Fig. 4.** Comparison of the daily evolution of ISO height with original height on (a) 1 July 1985, (b) 6 July 1985, (c) 11 July 1985, (d) 16 July 1985, (e) 16 June 1998, (f) 1 July 1998, (g) 11 July 1998, and (h) 21 July 1998. The ISO height (m) is denoted by solid lines (with only the parts > 0 in 1985, and the reverse in 1998) and the original height (10 m) by dashed lines.

the band-pass filtering of 2–7 yr (Fig. 5a) and low-pass filtering of 9 yr (Fig. 5b) on the two data series, respectively. The results of the 2–7-yr band-pass filtering show that the power spectra (the solid curve in Fig. 5a) of the 850-hPa  $v$  ISO averaged in the subtropical northwestern Pacific are stronger during the El Niño period, and weaker during the La Niña period. The correlation of the wavelet power spectra of the ISO and Niño-3.4 index (shadow in Fig. 5) reaches 0.22, passing the  $t$ -test at the 0.01 confidence level. The wavelet power spectra (dotted curve in Fig. 5a) of the 850-hPa  $v$  ISO averaged in the subtropical northeastern Pacific ( $20^{\circ}$ – $30^{\circ}$ N,  $180^{\circ}$ – $130^{\circ}$ W) are not obviously related to ENSO cycles. The 9-yr low-pass filtering results show that the correlation between the  $v$  ISO power spectrum averaged in the subtropical northwestern Pacific (solid curve in Fig. 5b) and Niño-3.4 index reaches  $-0.32$ , and the correlation between the  $v$  ISO power spectrum averaged in the subtropical northeastern Pacific (dotted curve in Fig. 5b) and Niño-3.4 index reaches 0.26, both passing the  $t$ -test at the 0.01 confidence level. Consequently, it is inferred that the power of the  $v$  ISO in the subtropical

northwestern Pacific has a positive correlation with the Niño-3.4 index at the ENSO cycle time scale, but the  $v$  ISO activities in the subtropical northeastern Pacific are not obviously correlated with Niño-3.4 index. Moreover, on the interdecadal time scale, the Niño-3.4 index has a coherent fluctuation relation with the  $v$  ISO power in the subtropical northeastern Pacific, and an opposite fluctuation relation with the  $v$  ISO power in the subtropical northwestern Pacific.

## 5. Summary and discussion

The atmospheric ISO activities over the subtropical northern Pacific are closely correlated with the summer precipitation anomaly in the subtropical eastern Asia. In this paper, the basic climate characteristics of the ISO of  $v$  over the subtropical northern Pacific are studied, and some issues meriting in-depth research and discussion are initiated. The study draws the main conclusions as follows:

(1) A two-dimensional space-time spectrum analysis on the daily variables such as  $u$ ,  $v$ , and  $h$  in each year of 1958–2002 has shown that the climatic

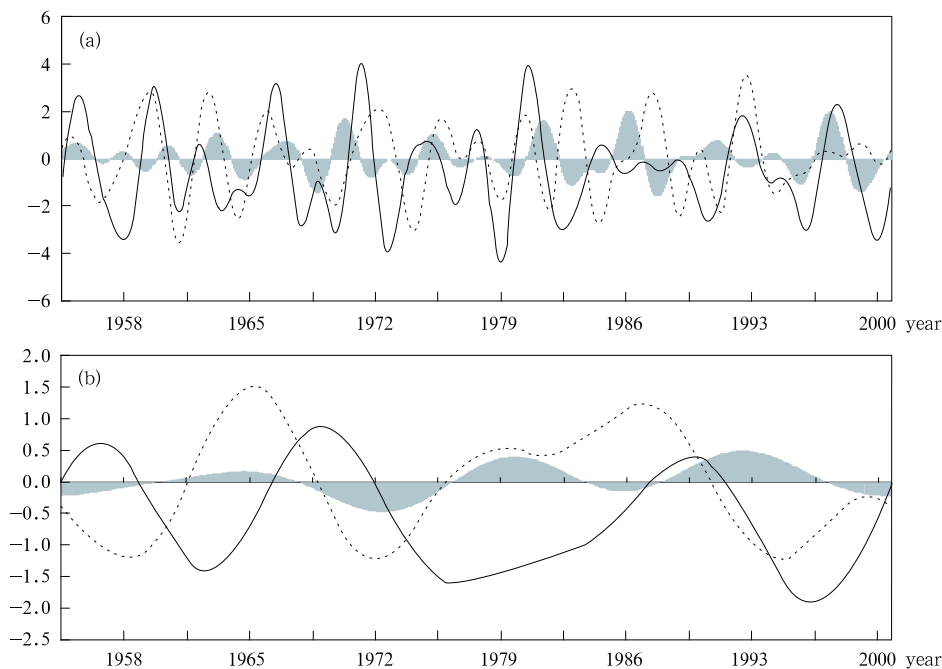


**Fig. 5.** Filtering analyses for the monthly ISO power spectra ( $10^{-1} \text{ m}^2 \text{ s}^{-2}$ ) of the 850-hPa  $v$  separately averaged in the northwestern Pacific (solid curve) and northeastern Pacific (dashed curve), and SST anomalies (shaded;  $^{\circ}\text{C}$ ) in Niño-3.4 region during 1958–2000 from the (a) 2–7-yr band-pass filter and (b) 9-yr low-pass filter. The northwestern Pacific refers to the area of  $20^{\circ}$ – $30^{\circ}$ N,  $110^{\circ}$ – $170^{\circ}$ E, and the northeastern Pacific  $20^{\circ}$ – $30^{\circ}$ N,  $180^{\circ}$ – $130^{\circ}$ W.

characteristics of ISO (30–60 days) of  $v$  from 30°S to 60°N is very different from those of other elements ( $u$ ,  $h$ ). The percentage of the ISO spectrum energies to the sum of spectrum energies of all waves (i.e., the ratio of ISO variance to total variance) for  $v$  is very low in the equator, but significantly high in the subtropics and midlatitudes. As the daily series in each year and the grid series along a certain latitude are concerned, the variance ratio of the  $v$  ISO in the subtropics and midlatitudes can be over 10%.

(2) The daily ISO evolution over the subtropical areas from East Asia to northern Pacific indicates that ISO is weak and indistinct in the atmospheric circulation at the beginning of the summer heavy rainfall event, but ISO features can turn to be significant later on. So the ISO energy can form the main part of the total energy of the atmosphere in a special synoptic event, and the ISO evolution may even influence the trend of the circulation development.

(3) For a 43-yr mean state, in the region from the subtropical East Asia to northwestern Pacific, the activity of ISO for 850-hPa  $v$  is the strongest in summer, slightly weaker in spring and autumn, and the weakest in winter, while in the subtropical northeastern Pacific the situation is reversed, where the ISO activity is the strongest in winter, and slightly weaker in spring and autumn, and the weakest in summer. Meanwhile, the ISO activity is rather weak in the eastern Asia between 30° and 45°N for the whole year.

(4) In the subtropical zone south of 30°N, the space-time spectral energy of the  $v$  ISO is mainly concentrated on wave numbers 5–6, while the energy over the subtropical zone north of 30°N is mainly concentrated on the wave numbers 4–5. So the propagating speeds of the ISO in the subtropical zones south and north of 30°N are different.

(5) During 1958–2000, the  $v$  ISO activity at 850 hPa over the subtropical northern Pacific has obvious interannual and interdecadal variations. Over the coastal areas of East Asia, the ISO activity is considerably strong during 1958–1976, obviously weak during 1976–1990, and the strongest during 1991–2000. In terms of interannual variations, the ISO changes in the northwestern Pacific contain appreciable in-phase

ENSO signals, but they are out of phase with the Niño-3.4 index changes on the interdecadal time scale. Does this mean that the influence of ENSO on the atmosphere is opposite to the interdecadal change of the atmospheric ISO over the subtropics? In other words, do the sea surface temperature changes have an inverted regulating effect on the long-term trend of the atmospheric ISO over the subtropics? This would be worthy of further studies.

## REFERENCES

- Anderson, J. R., and R. D. Rosen, 1983: Latitude-height structure of 40–50-day variations in atmospheric angular momentum. *J. Atmos. Sci.*, **40**(6), 1584–1591.
- Chen Longxun and Xie An, 1988: Westward propagating low-frequency oscillation and its teleconnection in the Eastern Hemisphere. *Acta Meteor. Sinica*, **2**(3), 300–312.
- Chen Longxun, Zhu Congwen, Wang Wen, et al., 2001: Analysis of characteristics of 30–60-day low frequency oscillation over Asia during 1998 SCSMEX. *Adv. Atmos. Sci.*, **18**(4), 623–638.
- Chen Xingyue, Wang Huijun, and Zeng Qingcun, 2000: *Atmospheric Intraseasonal Oscillation and Its Interannual Variation*. China Meteorological Press, Beijing, 15–22.
- Dickey, J. O., M. Ghil, and S. L. Marcus, 1991: Extratropical aspects of the 40–50-day oscillation in length of day and atmospheric angular momentum. *J. Geophys. Res.*, **96**(D12), 22643–22658.
- Dong Min, Zhang Xingqiang, and He Jinhai, 2004: A diagnostic study on the temporal and spatial characteristics of the tropical intraseasonal oscillation. *Acta Meteor. Sinica*, **62**(6), 822–830. (in Chinese)
- Ghil, M., and K. Mo, 1991: Intraseasonal oscillations in the global atmosphere. Part I: Northern Hemisphere and tropics. *J. Atmos. Sci.*, **48**(5), 752–779.
- Han Rongqing, Li Weijing, and Dong Min, 2006: Impacts of 30–60-day oscillations over the subtropical Pacific on the East Asian summer rainfall. *Acta Meteor. Sinica*, **20**(4), 459–474.
- Hayashi, Y., 1982: Space-time spectral analysis and its application to atmospheric waves. *J. Meteor. Soc. Japan*, **60**(1), 156–171.
- He Jinhai and Yang Song, 1992: Meridional propagation of East Asian low frequency oscillation and mid-

- latitude low-frequency waves. *Acta Meteor. Sinica*, **50**(2), 190–198. (in Chinese)
- Hsu, H. H., B. J. Hoskins, and F. -F. Jin, 1990: The 1985/86 intraseasonal oscillation and the role of extratropics. *J. Atmos. Sci.*, **47**(7), 823–839.
- Huang Jiayou and Li Huang, 1984: *The Wave Spectrum Analysis of Meteorology*. China Meteorological Press, Beijing, 254–300.
- Jin, F-F., and M. Ghil, 1990: Intraseasonal oscillations in the extra-tropics: Hopf bifurcation and topographic instabilities. *J. Atmos. Sci.*, **47**(24), 3007–3022.
- Ju Jianhua, Sun Dan, and Liu Junmei, 2007: The influence of the East Asian monsoon stream on the large scale precipitation course in eastern China. *Chinese J. Atmos. Sci.*, **31**(6), 1129–1139. (in Chinese)
- Kalnay, E., M. Kanamitsu, R. Kistler, et al., 1996: The NCEP/NCAR 40-year reanalysis project. *Bull. Amer. Meteor. Soc.*, **77**(3), 437–471.
- Krishnamurti, T. N., and S. Gadgil, 1985: On the structure of the 30- to 50-day mode over the globe during FGGE. *Tellus*, **37A**, 336–360.
- Li Chongyin, 1992: An analytical study on the precipitation in the flood period over Huabei area. *Acta Meteor. Sinica*, **50**(1), 41–49. (in Chinese)
- , 1993: *Atmospheric Low-Frequency Oscillation*. China Meteorological Press, Beijing, 3–6; 84–87.
- Li Guilong and Li Chongyin, 1998: Activity of atmospheric intraseasonal oscillation and El Niño. *Journal of Tropical Meteorology*, **14**(1), 54–62. (in Chinese)
- Liebmann, B., and D. L. Hartmann, 1984: An observational study of tropical-midlatitude interaction on intraseasonal time scales during winter. *J. Atmos. Sci.*, **41**(23), 3333–3350.
- Madden, R. A., and P. R. Julian, 1971: Detection of a 40-50-day oscillation in the zonal wind in the tropical Pacific. *J. Atmos. Sci.*, **28**(5), 702–708.
- , and —, 1972: Description of global scale circulation cells in the tropics with 40–50-day period. *J. Atmos. Sci.*, **29**(6), 1109–1123.
- Magana, V., and M. Yanai, 1991: Tropical-midlatitude interaction on the time scale of 30 to 60 days during the northern summer of 1979. *J. Climate*, **4**(2), 180–201.
- Murakami, T., 1988: Intraseasonal atmospheric teleconnection patterns during the Northern Hemisphere winter. *J. Climate*, **1**(2), 117–131.
- Simmons, A. J., J. M. Wallace, and G.W. Branstator, 1983: Barotropic wave propagation and instability, and atmospheric teleconnection patterns. *J. Atmos. Sci.*, **40**(6), 1363–1392.
- Sun Guowu and Chen Baode, 1988: The atmospheric intra-seasonal oscillations and its meridional propagations over Tibetan Plateau. *Chinese J. Atmos. Sci.*, **12**(3), 250–256. (in Chinese)
- Torrence, C., and G. Compo, 1998: A practical guide to wavelet analysis. *Bull. Amer. Meteor. Soc.*, **79**(1), 61–78.
- Xu Xiangde, Zhang Xuejin, and Chen Lianshou, 1999: The characteristics of LFO propagation dynamics on the Tibetan Plateau. *Theoretical Advances in the Second Scientific Experiment of Tibetan Plateau*. China Meteorological Press, Beijing, 162–168.